Catalytic Oxidation of a Diesel Soot Formed in the Presence of a Cerium Additive. II. Temperature-Programmed Experiments on the Surface-Oxygenated Complexes and Kinetic Modeling

ARTICLE *in* ENERGY & FUELS · DECEMBER 2004

Impact Factor: 2.79 · DOI: 10.1021/ef049840f

4 AUTHORS, INCLUDING:

Abdouelilah Hachimi
Saudi Basic Industries Corporation (SABIC)
9 PUBLICATIONS **28** CITATIONS

SEE PROFILE

Catalytic Oxidation of a Diesel Soot Formed in the Presence of a Cerium Additive. II. Temperature-Programmed Experiments on the Surface-Oxygenated Complexes and Kinetic Modeling

Régis Vonarb,[†] Abdouelilah Hachimi,[‡] Emmanuel Jean,[†] and Daniel Bianchi*[,‡]

Faurecia Systèmes d'échappements, Advanced Engineering, Diesel Exhaust After-Treatment Bois sur prés, 25 550 Bavans, France, and Laboratoire d'Application de la Chimie à l'Environnement (LACE), UMR 5634, Université Claude Bernard, Lyon-1, Bat. Raulin, 43 Bd du 11 Novembre 1918, 69622 Villeurbanne, France

Received July 8, 2004. Revised Manuscript Received October 19, 2004

Two diesel soots formed in a engine/exhaust line by using a fuel that contained 350 ppm (by weight) of sulfur with and without a cerium-based additive (diesel soots denoted Cec-DS and nc-DS, respectively) are studied (i) via temperature-programmed experiments in the temperature range of 300−1300 K and (ii) adsorption of O_2, CO, and CO_2 at several adsorption temperatures (T_a). It is shown that, during the linear increase of temperature in a helium flow (a procedure denoted as the He−Temperature Programmed Experiment, He-TPE), the "as-prepared" Cec-DS soot leads to the detection of a high CO_2 peak, with a maximum at $T_m = 905$ K, which is not observed on nc-DS. After the treatment of Cec-DS at 1200 K in helium, the adsorption of O_2 at $T_a < 660$ K leads, during the successive He-TPE, to observations similar to that on the freshly prepared soot, showing that the characteristic CO_2 peak is not linked to the formation of a particular surface-oxygenated complex (SOC), because of the experimental conditions of the engine/exhaust line. This CO_2 peak is ascribed to the oxidation of SOCs by oxygen species coming from the cerium-containing particles. A kinetic modeling of the observations during He-TPE is presented as a first step of a microkinetic approach of the soot oxidation. Three main surface elementary steps are considered: (i) decomposition of the cerium-containing particles (identified as cerium sulfate, $Ce_2(SO_4)_3$, in the as-prepared soot), which provides oxygen species O_s to the soot; (ii) the oxidation of the SOCs into CO_2 by the O_s species; and (iii) the desorption of the SOCs as CO. The kinetic model gives theoretical CO_2 and CO productions that are consistent with the experimental observations for a set of activation energies that leads to the conclusion that it is the decomposition of the cerium-containing particles that controls the formation of the CO_2 peak during the He-TPE. This kinetic model is (i) compared to literature data on the calcium-catalyzed gasification of carbon materials and (ii) used to suggest an orientation for the oxidation of diesel soots at lower temperatures.

1. Introduction

An attractive solution to eliminate the emission of the soot produced by diesel vehicles is to trap the particles on specific filters (i.e., SiC filter), followed by periodic oxidative regenerations to prevent a pressure increase in the exhaust line. To decrease the temperature of the regeneration significantly to protect the engine filter, organometallic compounds (i.e., cerium-based) can be added to the fuel. This oxidation of the soots is very similar to a classical gas/solid heterogeneous catalysis,[1] and there is a clear analogy in the vocabulary used to describe the elementary steps involved in the reaction such as active sites and adsorption rate of O_2.[1,2] Neeft et al.[3] and Stanmore et al.[1] have noted that there is a limited number of detailed studies on the kinetic of the soot oxidation that are mainly dedicated to formal kinetic approaches. Considering the similarity with gas/solid catalysis, a microkinetic approach[4] of the soot oxidation is developed[5] to obtain more insight on the reaction, as recently performed for the CO/O_2 reaction on Pt/Al_2O_3.[6,7] The first step of this approach consists of adopting a plausible mechanism for the reaction, to fix the elementary steps of interest, which are then characterized by experimental procedures associated with kinetic modeling. We have selected[5] the unified

* Author to whom correspondence should be addressed. E-mail: daniel.bianchi@univ-lyon1.fr.
[†] Diesel Exhaust After-Treatment Bois sur prés.
[‡] Laboratoire d'Application de la Chimie à l'Environnement (LACE).

(1) Stanmore, B. R.; Brilhac, J. F.; Gilot, P. *Carbon* **2001**, *39*, 2247−2268.
(2) Moulijn, J. A.; Kapteijn, F. *Carbon* **1995**, *33*, 1155−1165.
(3) Neeft, J. P. A.; Nijhuis, T. X.; Smakmann, E.; Makkee, M.; Moulijn, J. A. *Fuel* **1997**, *76*, 1129−1136.
(4) Dumesic, J. A., et al. *The Microkinetics of Heterogeneous Catalysis*; ACS Professional Reference Book; American Chemical Society: Washington, DC, 1993.
(5) Retailleau, L.; Vonarb, R.; Perrichon, V.; Jean, E.; Bianchi, D. *Energy Fuels* **2004**, *18*, 872−882
(6) Bourane, A.; Bianchi, D. *J. Catal.* **2002**, *209*, 114−125.
(7) Bourane, A.; Bianchi, D. *J. Catal*. **2001**, *202*, 34−44.

10.1021/ef049840f CCC: $30.25
Published on Web 12/08/2004

mechanism proposed for the noncatalytic and catalytic oxidation of carbonaceous materials.[2,8] The key surface elementary steps of this kinetic model are the adsorption of O_2 on surface-defect sites (denoted as C_f, CC_f, or C_nCC_f[5]) to form stable surface oxygen complexes (SOCs), according to[1,8]

$$\text{Step S1:} \quad C_nCC_f + \frac{1}{2}O_2 \leftrightarrows C_nCC_f(O) \quad \text{(equilibrium)} \quad (1)$$

These stable $CC_f(O)$ species react with oxygen to form unstable oxygen complexes $C(O)C_f(O)$, according to the elementary step[2,8]

$$\text{Step S2:} \quad C_nCC_f(O) + \frac{1}{2}O_2 \leftrightarrows C_nC(O)C_f(O) \quad \text{(equilibrium)} \quad (2)$$

The decomposition of the $C(O)C_f(O)$ species operates the oxidation of the carbon material, according to two elementary steps:[2,8]

$$\text{Step S3:} \quad C_nC(O)C_f(O) \rightarrow C_nC_fO + CO \quad \text{(fast)} \quad (3)$$

$$\text{Step S4:} \quad C_nC_f(O) \rightarrow C_{n-1}CC_f + CO \quad \text{(slow)} \quad (4)$$

An oxygen adsorption step (step S0) is also considered to produce $CC_f(O)$, slightly modifying steps S1 and S2. Chen and Yang[9] considered that $C_f(O)$ and $C(O)$ correspond to two distinct SOC species, such as semiquinone-type and off-plane oxygen, respectively. The formation of CO_2 is envisaged as the product of a sequential oxidation reaction.[2,8] The role of a catalyst during the soot oxidation is to favor either the O_2 adsorption (step S0) or/and the formation of the SOCs, without profoundly changing the kinetic mechanism: i.e., the activation energy of reaction is not affected significantly.[2]

This plausible mechanism supports our microkinetic approach[5] of the oxidation of a diesel soot formed with an engine using a commercial fuel (350 ppm in weight of sulfur) with a cerium additive (DPX-9 from Rhodia). In the first part of this work,[5] it has been shown that the cerium fraction is constituted of well-dispersed cerium(III) sulfate ($Ce_2(SO_4)_3$, not detected by XRD) and CeO_2 particles (average diameter of 23 nm). The decomposition of the sulfate seems to be a key step of the catalytic oxidation on the soots, whereas the CeO_2 particles do not seem to be strongly involved in the process.[5] The present study is dedicated to the characterization of the surface elementary steps of the oxidation of the cerium-catalyzed soot, using experiments in the transient regime associated with the kinetic modeling of the observations.

2. Experimental Section

2.1. Preparation and Characterization of the Diesel Soots. The diesel soots were obtained on an engine test bench fitted with a Volkswagen 1.9-L engine (81 kW, 225 N m at 1700 rpm). A fuel that contained 350 ppm of sulfur was used (i) without any additive, providing a noncatalyzed soot (denoted as nc-DS), and (ii) with a cerium-based additive (DPX-9 from Rhodia, 50 ppm (by weight) in the fuel), providing a catalyzed soot (denoted by Cec-DS). The soots were collected using SiC filters (200 cpsi, 5′ 66″ × 6′, 2.5 L) positioned in the exhaust line with an engine speed of 2500 rpm and load of 50 N m (the temperature of the filter was ∼493 K). These conditions limit the amount of volatile organic compounds (VOCs) in the soot and increase its cerium content.[10] The VOCs of DS soots are mainly (at least 95%) due to unburned lubricating oil,[11] whereas the oxidation of a fraction of SO_2 to SO_3 leads to the presence of sulfuric acid.[12] A commercial model DS soot (Printex U, from Degussa) has been used for comparison with Cec-DS and nc-DS. The characterizations of the soots have been described in detail in Part I,[5] and the parameters of interests for the present study are indicated in Table 1. In particular, it has been shown[5] that the cerium in Cec-DS is present as (i) CeO_2 particles, as detected by X-ray diffractometry (XRD) (average diameter of 23 nm), and (ii) well-dispersed cerium sulfate ($Ce_2(SO_4)_3$, as determined via susceptibility measurements (abbreviation MS.s): 49% of the cerium content). The characterizations of Printex-U are consistent with literature data.[13]

Table 1. Characterizations of the Three Diesel Soots

characterization	Printex U	Soot nc-DS	Soot Cec-DS
elemental analysis			
carbon (wt %)	92.6	82.6	64.1
oxygen (wt %)	3.2	6.3	12.4
sulfur (wt %)		1.02	2.7
cerium (wt %)			12.1
gravimetric analysis			
volatile matter (wt %)	5	5	4
ash (wt %)	$\sim 2 \times 10^{-2}$	$\sim 2 \times 10^{-2}$	18
BET surface area[a] (m^2/g)	95	179	239
$Ce_2(SO_4)_3$[b] (% Ce)			49

[a] After a vacuum pretreated at 473 K (2 h). [b] Susceptibility magnetic measurements.

2.2. Analytical Procedure. The analytical system has been described in detail previously.[14] Mainly, various valves allowed us to perform controlled switches between regulated gas flows in the range of 100−1000 cm^3/min (at the atmospheric pressure), which passed through the carbon material (mass in the range of 10−300 mg) contained in a quartz microreactor (volume of ∼1.1 cm^3). The gas composition (molar fractions) at the outlet of the reactor was determined using a quadrupole mass spectrometer (with an analysis frequency of 0.66 Hz) after a calibration procedure with gas mixtures of known compositions (the accuracy was dependent on the complexity of the gas mixture: the range is 2%−10%). The temperature was simultaneously recorded, using a small K-type thermocouple (diameter $\Phi = 0.25$ mm) that was inserted into the sample. This analytical system allowed to study (i) the adsorption of a gas G (i.e., G = O_2, CO, or CO_2) at several adsorption temperatures T_a (using *x*% G/*y*% Ar/He; Ar was a tracer, showing the beginning of the consumption of G), (ii) isothermal oxidation, and (iii) temperature-programmed experiments (denoted as TPEs; $\beta = 50$ K/min). For solid catalysts, TPE is a general abbreviation of well-defined experiments with particular acronyms:[15] TPD is used for either desorption of adsorbed species or decomposition of supported particles in a

(8) Chen, S. G.; Yang, R. T.; Kapteijn, F.; Moulijn, J. A. *Ind. Eng. Chem. Res.* **1993**, *32*, 2835−2840.
(9) Chen, S. G.; Tang, R. T. *Energy Fuels* **1997**, *11*, 421−427.
(10) Stratakis, G. A.; Stamatelos, A. M. *Combust. Flame* **2003**, *132*, 157−169.
(11) Sakurai, H.; Tobias, H. J.; Park, K.; Zarling, D.; Docherty, K. S.; Kittelson, D. B.; McMurry, P. H.; Ziemann, P. J. *Atmos. Environ.* **2003**, *37*, 1199−1210.
(12) Tobias, H. J.; Beving, D. R.; Ziemann, P. J.; Sakurai, H.; Zuk, M.; McMurry, P. H., Zarling, D.; Waytulonis, R.; Kittelson, D. B. *Environ. Sci. Technol.* **2001**, *35*, 2233−2243.
(13) Neeft, J. P. A.; Makkee, M.; Moulijn, J. A. *Fuel* **1998**, 77, 111−119.
(14) Bourane, A.; Bianchi, D. *J. Catal.* **2002**, *209*, 126−134.

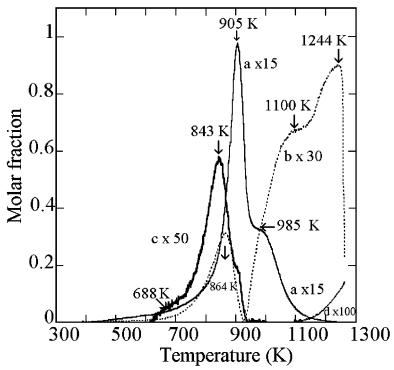

Figure 1. He-TPE (50 K/min) of the "as-prepared" Cec-DS soot: CO_2 (curve a), CO (curve b), SO_2 (curve c), and H_2 (curve d).

helium flow, TPO is used for oxidation in the presence of O_2 (i.e., x% O_2/He flow), and TPSR is used for surface reaction between strongly adsorbed species in a helium flow. A TPE may involve TPD, TPSR, and TPO simultaneously, leading to a complex spectrum (several gases are produced). In the present study, TPEs with Cec-DS were performed in a helium flow (denoted He-TPEs), and they were due to (i) the decomposition of cerium-containing particles (TPD), (ii) the desorption of SOCs (TPD), and (iii) the TPSR between the SOCs and the oxygen species formed by the decomposition of the cerium-containing particles. He-TPE with nc-DS and Printex U were only due to desorption of the adsorbed species, and they are conventionally denoted TPD in this presentation. The He-TPE and O_2 (or CO or CO_2) adsorption were performed as follows: a mass of soot (in the range of 0.1−0.3 g), slightly compressed to decrease its apparent volume, was introduced into the microreactor and heated in helium to a temperature of $T \leq$ 523 K (according to the soot) for 2 h, to remove the VOCs. The sample then was cooled to 300 K in helium, and the temperature was increased (50 K/min, He-TPE, $T <$ 1300 K) to characterize the soot coming from the preparation. The solid then was cooled to the adsorption temperature (T_a, in the range of 173−660 K), and a switch from helium to 1% G/1% Ar/He (G = O_2, CO, or CO_2, with a flow rate of 100−250 cm^3/min) was performed to adsorb G for a duration t_a. The sample was cooled (or heated at T_a = 173 K) in the presence of G to room temperature and, after a purge in helium, a He-TPE was performed to characterize the SOCs formed by the adsorption of G. Adsorption/He-TPE cycles were performed on the same sample.

3. Results

3.1. He-TPE of the "As-Prepared" Soots. These results have been described in more detail in Part I.[5] However, they are summarized to facilitate the presentation of the present study. Figure 1 gives the He-TPE spectrum observed on Cec-DS (after the desorption of the VOCs at 500 K), showing (i) a SO_2 peak (curve c in Figure 1) at T_m = 843 K that is associated with a broad shoulder at lower temperatures (∼688 K; total amount of 205 μmol/g); (ii) a CO peak (curve b in Figure 1, 327 μmol/g) at T_m = 864 K, desorbing in parallel with SO_2; (iii) a well-defined CO_2 peak at T_m = 905 K (curve a in Figure 1) that is associated with a shoulder at a higher temperature (∼985 K; total amount of CO_2 = 2174 μmol/g); and (iv) two broad overlapped peaks of CO at T_m = 1100 and 1244 K (see curve b in Figure 1, 2107 μmol/g). At desorption temperatures of $T_d >$ 1100 K, a small amount of hydrogen production is detected (53 μmol/g; see curve d in Figure 1). These different peaks are linked to TPD and TPSR processes, and, according to the Brunauer−Emmett−Teller (BET) surface area (Table 1), their amounts are compatible with adsorbed surface species.[5] The oxygen mass balance represents ∼11.5 wt % of the soot, which is consistent with the elemental analysis (Table 1). The amount of SO_2 is lower during the He-TPE than that expected from the elemental analysis (Table 1). This is due to the formation, in the course of the He-TPE, of a very stable sulfur- and cerium-containing compound that is tentatively ascribed[5] to oxysulfide (i.e., Ce_2O_2S) or sulfides, according to literature data.[16,17] Considering the change in the nature of the well-dispersed cerium-containing particles during the experiments (He-TPE in helium and O_2 adsorption), we adopt, to simplify the presentation, the notation $Ce_xO_yS_z$ for the cerium fraction of the Cec-DS (where x, y, and z change according to the experiments). The TPD of nc-DS leads to a more-complex spectrum than that on Cec-DS.[5] There is a SO_2 desorption (132 μmol/g) at 585 K, followed by at least four strongly overlapped CO_2 peaks—at 680, 840, 935, and 1010 K (total amount of 1100 μmol/g)—associated with a broad CO production, with a maximum at 990 K and two shoulders at ∼750 and 850 K (total amount of 1438 μmol/g). Hydrogen production (127 μmol/g) is detected for $T_d >$ 940 K. The oxygen mass balance indicates that the oxygen content of the soot is 5.9 wt %, in good agreement with the elemental analysis (see Table 1). The TPD of Printex U (after desorption of VOCs at 373 K) is similar to that on nc-DS.[5] There is a very small amount of SO_2 desorption at 580 K (3 μmol/g), similar to nc-DS, associated with several overlapped CO_2 peaks between 554 and 945 K (total amount of 237 μmol/g). A broad CO peak is observed from 600 to 1100 K, with a shoulder at ∼480 K (total CO production of 790 μmol/g). There is hydrogen production (273 μmol/g) at $T_d >$ 980 K. The oxygen mass balance indicates that the oxygen content of the soot is 2.0 wt %, in agreement with the elemental analysis (Table 1). The CO and CO_2 peaks of the TPD spectra of nc-DS and Printex U are in agreement with similar literature data on various carbon materials.[18−25] Several overlapped peaks of CO_2 and CO are observed, because of SOCs with activation energies of desorption in the range of 115−380 kJ/mol.[19,24] The more-stable SOCs mainly desorb as CO.[24−26] In Figure 1, the strong CO_2 peak at T_M = 905 K between the two CO peaks at 864 K, and $T >$ 1000 K is a characteristic of the Cec-DS soot. The intent of the

(15) Falconer, J. L.; Schwarz, J. A. *Catal. Rev. Sci. Eng.* **1983**, *25*, 141−227.
(16) Luo, T.; Vohs, J. M.; Gorte, R. J. *J. Catal.* **2002**, *210*, 397−404.
(17) Ferrizz, R. M.; Gorte, R. J.; Vohs, J. M. *Appl. Catal., B* **2003**, *43*, 273−280.
(18) Kyotani, T.; Zhang-Guo, Z.; Hayashi, S.; Tomota, A. *Energy Fuels* **1988**, *2*, 136−141.
(19) Du, Z.; Sarafin, A. F; Longwell, J. P. *Energy Fuels* **1990**, *4*, 296−302.
(20) Huttinger, K. J.; Nill, J. S. *Carbon* **1990**, *28*, 457−465.
(21) Brown, T. C.; Haynes, B. S. *Energy Fuels* **1992**, *6*, 154−159.
(22) Pan, Z.; Yang, R. T. *Ind. Eng. Chem. Res.* **1992**, *31*, 2675−2680.
(23) Marchon, B.; Tysoe, W. T.; Carrazza, J.; Heinemann, H.; Somorjai, G. A. *J. Phys. Chem.* **1988**, *92*, 5744−5749.
(24) Haydar, S.; Moreno-Castilla, C.; Ferro-Garcia, M. A.; Carrasco-Marin, F.; Rivera-Utrilla, J.; Perrard, A.; Joly, J. P. *Carbon* **2000**, *38*, 1297−1308.
(25) Szymanski, G. S.; Karpinski, Z.; Biniak, S.; Swiatkowski, A. *Carbon* **2002**, *40*, 2627−2639.
(26) Domingo-Garcia, M.; Lopez Garzon, F. J.; Perez-Mendoza, M. J. *J. Colloid Interface Sci*. **2002**, *248*, 116−122.

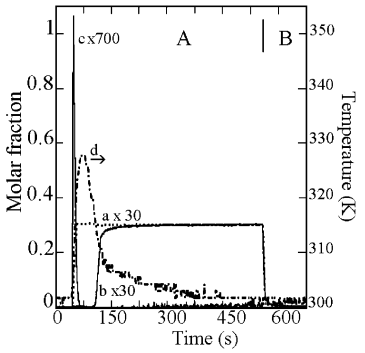

Figure 2. Adsorption of 1% O_2/1% Ar/He on Cec-DS at 303 K after a He-TPE: Ar (curve a), O_2 (curve b), CO (curve c), and temperature (curve d).

present study is to provide a kinetic modeling of these observations from a mechanism that involves surface elementary steps. In a first step, experiments have been performed to determine if the characteristics of the He-TPE of the "as-prepared" Cec-DS soot are linked to the presence of a particular SOC formed in the experimental conditions of the engine/exhaust line system (i.e., adsorption of a particular oxygenated carbonaceous species).

3.2. Oxygen Chemisorption on the Cec-DS at Several Adsorption Temperatures. The O_2 adsorption experiments are performed as follows. After the He-TPE of the "as-prepared" soot ($T_{max} \approx 1100$ K), the sample is cooled to T_a and a He → 1% O_2/1% Ar/He (100 cm^3/min) switch is performed for a duration t_a ($t_a = 12$ min for T_a values that lead to simultaneous O_2 adsorption and soot oxidation). For $T_a = 302$ K, Figure 2 shows that there is a strong exothermic ($\Delta T_{max} = 27$ K) O_2 consumption. The total amount of O_2 consumption ($Q_{O_2} = 156$ μmol/g) is obtained by

$$Q_{O_2} = \int_0^{t_a} (\text{curve a} - \text{curve b}) \frac{F}{W} \, dt \qquad (5)$$

where F is the total molar flow rate and W is the weight of the sample. Note that the argon signal (curve a in Figure 2) increases simultaneously with temperature T. During the first seconds of the introduction, there is a sharp and small amount of CO production (3 μmol/g). The 1% O_2/1% Ar/He → He switch in region B in Figure 2 leads to a small amount of O_2 desorption (~3 μmol/g), probably because of the micropores of the soot, showing that the main part of Q_{O_2} is irreversibly adsorbed: $Q_{O_2,ir} = 153$ μmol/g. After a He-TPE of the as-prepared soot at a higher temperature ($T_{d,max} = 1300$ K), $Q_{O_2,ir} = 248$ μmol/g at $T_a = 300$ K. The MS.s have shown that the Ce^{3+} ions present in the as-prepared soot and quantified as $Ce_2(SO_4)_3$ (Table 1) do not react with O_2 at 300 K. However, they are transformed during He-TPE to Ce^{3+} ions that are oxidized to Ce^{4+} ions by adsorption/reaction with O_2 at 300 K.[5] This Ce^{3+}→ Ce^{4+} transformation consumes 103 μmol of O_2/g independently of the adsorption temperature,[5] indicating that the O_2 adsorption at 302 K is associated with the formation of a small amount of SOC, according to reaction 1: $Q_{SOC} = (150 - 103) \times 2 = 94$ μmol/g, probably at the proximity of the cerium-containing particles. This Q_{SOC} value is strongly lower than that on the as-prepared soot, because of the difference in the experimental conditions

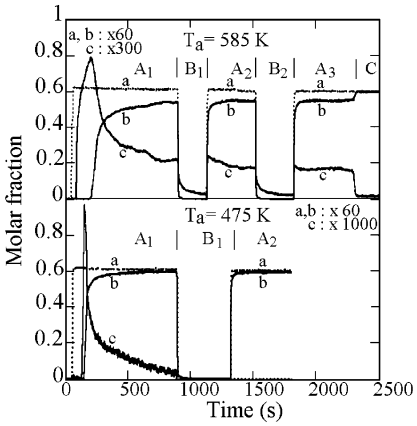

Figure 3. Isothermal adsorption of 1% O_2/1% Ar/He on Cec-DS desorbed at 1100 K at an adsorption temperature of T_a = 475 K (bottom) and 585 K (top): Ar (curve a), O_2 (curve b), and CO_2 (curve c) (CO not shown). Region A_i denotes O_2 adsorption, region B_i represents isothermal desorption, and region C_i denotes the cooling stage in O_2.

(soot formation, O_2 partial pressure, and adsorption temperature). Oxygen adsorption at $T_a > 300$ K confirms that more SOCs are formed. For $T_a = 390$ K (results not shown), the observations are similar to Figure 2, with $\Delta T_m = 27$ K and $Q_{O_2,ir} = 204$ μmol/g, showing an increase in Q_{SOC} (to $Q_{SOC} = 202$ μmol/g). The adsorption of O_2 at $T_a = 173$ K (results not shown) also leads to an exothermic process ($\Delta T_m = 12$ K), indicating that the Ce^{3+}→ Ce^{4+} transformation is possible at this temperature (confirming the high reactivity of the reduced form of $Ce_xO_yS_z$). However, an oxygen mass balance cannot be performed at $T_a = 173$ K, because of the large amounts of O_2 and argon that are adsorbed in the micropores of the soot.

For $T_a > 473$ K, the O_2 adsorption is associated with CO_2 and CO productions, indicating that some SOC species can be oxidized in parallel to the O_2 adsorption. For instance, the bottom of Figure 3 shows the evolutions of the gas molar fractions during the He → 1% O_2/1% Ar/He switch at $T_a = 475$ K on Cec-DS soot after a He-TPE at 1100 K. During the first seconds of the exothermic O_2 consumption ($\Delta T_m = 26$ K), there is no CO_2 production: the oxygen consumption is due to the Ce^{3+} → Ce^{4+} transformation and the formation of the SOCs. A sharp CO_2 peak—14 μmol/g, with a decreasing exponential profile (associated with a small CO production: ~3 μmol/g (not shown))—then is observed, indicating that a small fraction of the SOCs either desorbs as CO_2 (assuming, for instance, a low activation energy of desorption) or are oxidized by O_2. The profile of the CO_2 production indicates that the soot oxidation is not sustained: highly reactive CC_f sites produced during He-TPE are irreversibly removed from the soot surface (these sites are not regenerated, according to reaction 4). The oxygen mass balance [O_2 consumption−(CO_2 + $^1/_2$CO) productions] indicates that $Q_{O_2,ir} = 318$ μmol/g at 475 K, confirming that the higher the T_a value, the higher the Q_{SOC} value (430 μmol/g). A helium purge (bottom of Figure 3, region B_1) indicates that there is no CO/CO_2 desorption, whereas the reintroduction of O_2 (bottom of Figure 3, region A_2) shows that there is no more significant O_2 adsorption. For $T_a = 585$ K, the top of Figure 3 (region A_1) shows that CO_2 is produced before the appearance of O_2 in the gas phase (total

consumption of O_2, because of the adsorption and the soot oxidation). The rate of the CO_2 production presents an exponential decreasing profile to a pseudo-stationary value, indicating that the soot oxidation is sustained at this temperature. The oxygen mass balance leads to $Q_{O_2,ir} = 387$ μmol/g, showing again that Q_{SOC} increases with T_a (568 μmol/g). A purge in helium (top of Figure 3, region B_1) leads to a small CO_2 desorption, whereas the reintroduction of O_2 (region A_2) reveals clearly that the O_2 consumption is now only due to the soot oxidation. After a new desorption (region B_2 in Figure 3), the introduction of O_2 (region A_3) shows that a stationary production of CO_2 is observed. Considering the accuracy of the measurements, the oxygen mass balance indicates that the O_2 consumption (O_2 molar fraction of 0.91×10^{-2}, as compared to 10^{-2} at the inlet of the reactor) is due to the CO_2 formation (CO_2 molar fraction 0.084×10^{-2}). This shows that the rate of accumulation of the SOCs is low at the steady state of the sustained oxidation at 585 K. The decrease in T_a (top of Figure 3, region C) shows that the reaction rapidly ceases: the O_2 molar fraction increases to the inlet molar fraction (0.01). Note that there is no O_2 adsorption during the decrease in T_a, indicating that there are no available C_f sites with a low activation energy of adsorption. For $T_a = 660$ K (results not shown), the observations are similar to $T_a = 585$ K. However, the soot oxidation proceeds with a high rate, which necessitates the use of a higher flow rate (250 cm^3/min) of 1% O_2/1% Ar/He to detect an O_2 molar fraction at the outlet of the reactor. The oxygen mass balance leads to $Q_{O_2,ir} = 620$ μmol/g, which confirms the increase of Q_{SOC} (1034 μmol/g) with T_a.

The O_2 adsorption on Cec-DS at several adsorption temperatures leads to the following conclusions: (i) the reactivity with O_2 of the reduced form of the $Ce_xO_yS_z$ is very high (observed at 173 K); (ii) SOCs can be formed at 300 K in the presence of cerium; (iii) the increase in T_a increases the value of Q_{SOC} (the oxygen adsorption is an activated process); (iv) for $T_a = 473$ K, a nonsustained soot oxidation is detected, in parallel with the O_2 adsorption (the highest reactive CC_f sites formed by the He-TPE of the soot at 1100 K are not regenerated by reaction 4); (v) the soot oxidation is sustained for $T_a > 585$ K, indicating that reaction 4 is operative; and (vi) Q_{SOC} increases with T_a, even for a sustained soot oxidation.

3.3. He-TPE after Adsorption of O_2 on Cec-DS at Several Adsorption Temperatures. The He-TPE spectra after the adsorption of 1% O_2/1% Ar/He at several T_a values, followed by a cooling stage in O_2, are shown in panels A (CO_2 and SO_2 peaks) and B (CO and SO_2 peaks) in Figure 4. After adsorption at 302 K, the He-TPE spectrum is characterized by a CO_2 peak (65 μmol/g) at 910 K, which is associated with two CO peaks (total amount of 42 μmol/g) at 850 K and $T > 1000$ K. In comparison to the amount of O_2 adsorbed as SOC species (47 μmol O_2/g), the oxygen mass balance during the He-TPE (65 + (42/2) = 86 μmol of O_2/g) clearly indicates that oxygen species from $Ce_xO_yS_z$ are involved in the CO_2 and CO peaks. This is consistent with the fact that the MS.s reveal a $Ce^{4+} \rightarrow Ce^{3+}$ transformation during the He-TPE after O_2 adsorption at 300 K.[5] It must be considered that, after adsorption of O_2, the

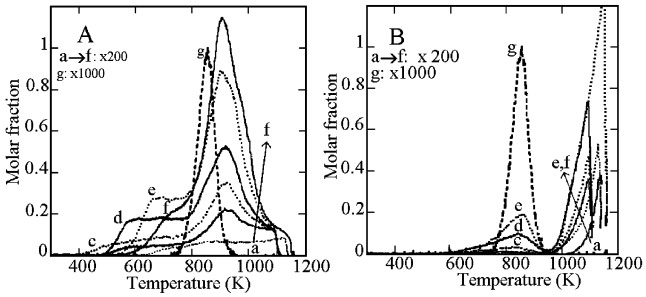

Figure 4. He-TPE after adsorption of O_2 on Cec-DS at several adsorption temperatures (T_a): (A) CO_2 and SO_2 productions and (B) CO and SO_2 production. $T_a = 173$ K (curve a), 303 K (curve b), 373 K (curve c), 457 K (curve d), 585 K (curve e), and 660 K (curve f); curve g denotes SO_2 at 660 K.

$Ce_xO_yS_z$ particles are an oxygen reservoir during the He-TPE: these oxygen species form new SOCs that desorb or/and oxidize the SOCs. The increase in Q_{SOC} with the increase in T_a (see Figures 2 and 3) is well-confirmed by the He-TPE. It can be observed in panels A and B of Figure 4 that the number and the profile of the CO and CO_2 peaks do not change with the increase in T_a: only the intensity of each peak increases (progressive transformation of similar CC_f sites). For $T_a > 570$ K, there is a SO_2 production at $T_d = 850$ K during the He-TPE: 113 μmol of SO_2/g for $T_a = 660$ K (curve g in Figure 4). For $T_a = 580$ K, the SO_2 peak corresponds to 7.5 μmol of SO_2/g (result not shown). For $T_a = 660$ K, the oxygen mass balance during the He-TPE (635 μmol/g of O_2) is consistent with the amount of O_2 adsorbed ($Q_{O_2,ir} = 620$ μmol/g). The comparison of the He-TPD spectrum for $T_a = 660$ K in panels A and B for Figure 4 with that of the as-prepared soot (Figure 1) shows that the profiles of CO, CO_2, and SO_2 peaks are very similar, indicating that they are formed by identical surface processes. This strongly suggests that the SOCs of the fresh Cec-DS soot are not linked to the adsorption of specific gaseous species in the engine/exhaust line. They are formed by the O_2 chemisorption at high temperatures (O_2 is in excess in the exhaust line). However, the value of Q_{SOC} is lower in Figure 4 for $T_a = 660$ K than in Figure 1: the first and second CO peaks are 37 and 413 μmol/g, respectively, and the CO_2 peak is 297 μmol/g. The impact of higher T_a values on Q_{SOC} cannot be studied with the microreactor, because the high oxidation rate, which is associated with the O_2 chemisorption, leads, on one hand, to a total O_2 consumption for low O_2 partial pressures (in homogeneity in the soot sample) and, on the other hand, to deep oxidation and ignition for high P_{O_2} values. The detection of the SO_2 peak in panels A and B in Figure 4 for $T_a \geq 580$ K indicates that the very stable reduced form of $Ce_xO_yS_z$ (i.e., oxysulfide, sulfide) that is formed during the He-TPE can be transformed to a new phase (i.e., a sulfate-like compound) that produces SO_2. It has been verified that sulfur remains in the soot after the He-TPE in Figure 4: a second O_2 adsorption at $T_a = 660$ K leads to a smaller SO_2 peak during the following He-TPE. The repetition of O_2 adsorption/He-TPE cycles on the same sample leads to a progressive decrease in the SO_2 production during the He-TPE. Note that, even after adsorption of O_2 at 173 K, there are small amounts of CO and CO_2 production (see spectra a in panels A and B in Figure 4), showing that either SOCs are formed at 173 K or, more probably,

that oxygen species of the oxidized $Ce_xO_yS_z$ particles form the SOCs during the He-TPE.

The main differences between the He-TPE spectra in Figures 1 and 4 are observed for $T < 700$ K. On the as-prepared Cec-DS soot (Figure 1), there are no distinct shoulders on the CO_2 peak at the opposite of the observations in Figure 4A. Moreover, Figure 4A shows that the increase in T_a has two main effects on the CO_2 production at $T_d < 700$ K: (i) the intensities of the overlapped CO_2 peaks increase for $T_a \leq 573$ K (increase in Q_{SOC}) (see curves a−c in Figure 4A) and (ii) for $T_a \geq 373$ K, the higher the T_a value, the higher the T value for the beginning of the CO_2 production (see curves c−f in Figure 4A). This indicates that the CC_f sites created during the He-TPE and allowing the formation of less-stable SOCs for $T_a < 573$ K are irreversibly removed from the surface by oxidation for $T_a > 573$ K (this process corresponds to the decreasing exponential profile of the CO_2 production during the first minutes of the O_2 adsorption in Figure 3). The data in Figure 4 confirm that the CC_f sites forming the less-stable SOCs are not regenerated by reaction 4, to sustain the soot oxidation. The sustained oxidation at $T_a > 585$ K (Figure 3) involves more-stable SOCs, which allow the regeneration of CC_f sites, according to reaction 4. For the microkinetic approach of the soot oxidation, this emphasizes the role of these stable SOCs and confirms the interest for a kinetic modeling of the processes involved in the He-TPE at $T > 600$ K.

3.4. Adsorption of CO and CO_2 on Cec-DS after He-TPE at 1200 K. These adsorptions have been studied considering the fact that the increase in Q_{SOC}, during O_2 adsorption at $T_a > 480$ K, may be tentatively associated to the readsorption of the CO and CO_2 formed by the soot oxidation on specific CC_f sites. The adsorptions have been performed using 1% CO (or 1% CO_2)/1% Ar/He. After adsorption at T_a, the solid is cooled in CO (or CO_2) to 300 K and, after a purge in helium, a He-TPE is performed (50 K/min) (only desorption processes are involved after the adsorption of CO and CO_2: the He-TPE is a conventional TPD). For $T_a = 300$ K (results not shown), a small amount of reversible CO adsorption (6 μmol/g) is observed, probably because of the micropores: there are no CO/CO_2 peaks during the following He-TPE. After the adsorption of CO at $T_a = 573$ K (Figure 5A), a He-TPE reveals small CO_2 ($T_M = 625$ K, ~2 μmol/g) and CO ($T_M = 697$ K and $T_M = 859$ K, ~7 μmol/g) peaks. These results show that (i) the CO adsorption does not contribute significantly to the observations after O_2 adsorption/oxidation on Cec-DS (Figure 4), and (ii) the CO adsorption on Cec-DS is a strongly activated process. At 300 K, the adsorption of CO_2 (84 μmol/g of CO_2) is slightly exothermic: $\Delta T \approx 3$ K (result not shown). The helium purge at 300 K leads to the desorption of 49 μmol/g of CO_2 (according to a decreasing exponential profile), which is probably linked to weakly adsorbed species in the micropores. The He-TPE (Figure 5B) performed before the total isothermal desorption at 300 K reveals a sharp CO_2 peak at 366 K that is due to the adsorption in the micropores. For $T_d > 400$ K, two broad CO_2 peaks at 445 and 520 K (~10 μmol/g) that are associated with a CO peak at 680 K (5 μmol/g) are observed. The He-TPE after adsorption of CO_2 at $T_a = 573$ K (see curves c and d in Figure 5B),

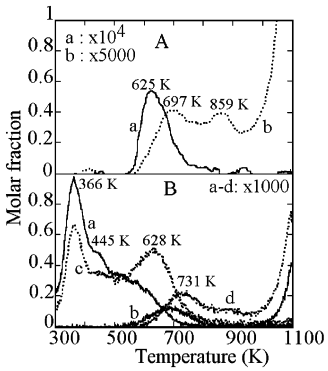

Figure 5. TPD after adsorption of CO and CO_2 at several adsorption temperatures on Cec-DS. Panel A shows CO_2 (curve a) and CO (curve b) after adsorption of 1% CO/1% Ar/He at $T_a = 573$ K. Panel B shows CO_2 and CO productions after adsorption of CO_2 at $T_a = 300$ and 573 K: CO_2, $T_a = 300$ K (curve a); CO, $T_a = 300$ K (curve b); CO_2, $T_a = 573$ K (curve c); and CO, $T_a = 573$ K (curve d).

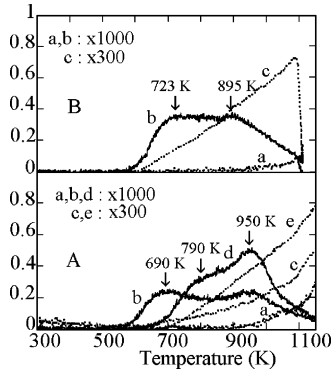

Figure 6. TPD after adsorption of 1% CO/1% Ar/He at several adsorption temperatures T_a on (A) nc-DS and (B) Printex U. Panel A shows CO production before and after adsorption of O_2 at 300 K (curve a); CO_2 production after $T_a = 573$ K (curve b); CO production after $T_a = 573$ K (curve c); CO_2 production after $T_a = 660$ K (curve d); and CO production after $T_a = 660$ K (curve e). Panel B shows CO production before and after adsorption of O_2 at 300 K (curve a); CO_2 production after $T_a = 573$ K (curve b); and CO production after $T_a = 573$ K (curve c).

followed by cooling the sample in CO_2, leads to a CO_2 peak at 366 K, because of the adsorption in the micropores, and two CO_2 peaks at 445 and 628 K (~20 μmol/g) are associated with two small CO peaks at 731 and 860 K (~11 μmol/g). It cannot be excluded that some peaks concern adsorbed species (i.e., carbonate) on the well-dispersed CeO_2 and $Ce_xO_yS_z$ particles. The Q_{SOC} values after adsorption at 573 K show that (i) readsorption of CO_2 cannot contribute significantly to the He-TPE observations after O_2 adsorption/oxidation on Cec-DS and (ii) the adsorption of CO_2 on Cec-DS is an activated process (excluding the adsorption in the micropores).

3.5. O_2 Chemisorption/Temperature-Programmed Desorption on nc-DS and Printex U Desorbed at 1200 K. There is no significant O_2 adsorption at 300 K on nc-DS desorbed in helium at 1200 K, and the TPD cannot be differentiated from that of the soot without any O_2 adsorption (see curve a in Figure 6A). At $T_a = 573$ K, the soot oxidation is observed in parallel with the O_2 chemisorption, leading to a CO_2 production with a decreasing exponential profile (results not shown,

similar to Figure 3). The oxygen mass balance indicates that $Q_{O_2,ir} = 130$ μmol/g (the formation of SOCs). The TPD spectrum of the SOCs (curves b and c in Figure 6A) indicates two overlapped CO_2 peaks, at $T_M = 690$ K and $T_M = 950$ K (total amount of 23 μmol/g), and a broad CO peak beginning at 600 K with several shoulders between 650 and 1150 K. For $T_a = 660$ K, the amounts of CO_2 and CO desorbed during the TPD increase, as shown in curves d (37 μmol/g of CO_2) and e, respectively, in Figure 6A. For the CO_2 production, it can be observed by comparison with $T_a = 573$ K that the peak at $T_M = 690$ K is eliminated while that at $T_M = 950$ K increases. This shows that, similar to Cec-DS, the more-reactive CC_f sites of nc-DS that form the less-stable SOCs are not regenerated by reaction 4 during the soot oxidation. There is no SO_2 production after the adsorption of O_2 at $T_a = 660$ K, indicating that the sulfur-containing species of the as-prepared soot are totally desorbed during the first TPD.

The adsorption of O_2 on Printex U leads to observations that are very similar to those on nc-DS. At $T_a = 300$ K, there is no significant adsorption and the TPD spectra cannot be differentiated from that observed without any O_2 adsorption (see curve a in Figure 6B). For $T_a > 573$ K, the oxidation of the soot is observed in parallel to the O_2 adsorption: there are CO_2 and CO productions with a decreasing exponential profile (as in Figure 3). The oxygen mass balance indicates that $Q_{O_2,ir} = 162$ μmol/g at $T_a = 573$ K and the TPD spectrum (Figure 6B) shows that the SOCs are very similar to those formed on nc-DS (Figure 6A): there are two overlapped CO_2 peaks at $T_M = 723$ K and $T_M = 895$ K (see curve b in Figure 6B; total amount of 35 μmol/g) that are associated with a broad CO peak beginning at 600 K (see curve c in Figure 6B). Clearly, nc-DS and Printex U present similar properties for the O_2 chemisorption, in agreement with the fact that Printex U is considered as a good model material of the diesel soot.

4. Discussion

4.1. Comparison of the He-TPE Spectra on the Three Soots with Literature Data. The CO and CO_2 peaks during the TPD of the as-prepared nc-DS and of the Printex U, as well as after O_2 adsorption (Figure 6), are consistent with the literature data on carbon solids.[18−26] Usually, there are several overlapped CO_2 peaks between 400 and 900 K, whereas CO is characterized by a broad peak from 400 to >1100 K with more-or-less distinct shoulders.[18−26] These peaks are ascribed to SOCs of different stabilities, such as those for CO_2 (carboxylic and lactones) and for CO at low temperatures (carbonyl, ketone, ester), whereas at $T > 600$ K, carboxylic anhydric, quinone, semiquinone, and pyrone are considered.[18−27] The desorption of the SOCs produces either CO or CO_2, except for the anhydride, which gives CO and CO_2.[27] On several carbon-containing solids, Haydar et al.[24] have shown that the E_d values of seven SOCs desorbing as CO_2 are in the range of 117−322 kJ/mol, whereas that of eight SOCs desorbing as CO are in the range of 142−376 kJ/mol. The observations on nc-DS and Printex U are consistent with these views:[18−27] there are weakly stable SOCs producing the CO_2 and CO peaks at low T_d values and strongly stable SOCs producing CO at high temperatures. For Cec-DS (see Figures 1 and 4), there is also a strong analogy with the literature data for several CO and CO_2 desorption peaks (i.e., CO_2 peaks at $T < 700$ K and the broad CO peak at high temperatures). In correlation with the soot oxidation, it has been shown that the less-stable SOCs formed by O_2 adsorption at low temperatures (desorbing as CO_2 in Figure 4) are irreversibly removed in the first seconds of the soot oxidation and do not participate to the sustained soot oxidation.

The particularities of the He-TPE of the as-prepared Cec-DS soot, because of the presence of $Ce_xO_yS_z$, are (i) the sharp CO_2 peak at $T_M = 905$ K appearing between the two CO peaks at $T_M = 864$ and $T_M = 1100$ K and (ii) the SO_2 desorption at $T_M = 843$ K detected in parallel with the CO peak at 864 K. This can be interpreted either by the formation of a specific SOC desorbing as CO_2 or by the oxidation of classical stable SOCs by oxygen species coming from $Ce_xO_yS_z$. The involvement of the oxidation reaction is supported by the fact that the CO_2 peak is observed at a temperature slightly higher than the SO_2 peak due to the $Ce_2(SO_4)_3$ decomposition.[5] In agreement with literature data, it has been shown[5] that the TPD (decomposition) of pure $Ce_2(SO_4)_3$ produces (i) parallel O_2 and SO_2 peaks at $T_m = 1140$ K with a SO_2/O_2 ratio of 3.1 and (ii) CeO_2 particles (MS.s) in agreement with

$$Ce_2(SO_4)_3 \rightarrow 2CeO_2 + 3SO_2 + O_2 \qquad (6)$$

During the He-TPE of Cec-DS, there is no O_2 production that is associated with the $Ce_2(SO_4)_3$ decomposition, indicating either that it is totally consumed by the soot oxidation or that the decomposition mechanism in the presence of soot is different than that of the pure sulfate solid. It has been shown that the amount of SO_2 production during the He-TPE of Cec-DS (Figure 1) is much less than that expected from elemental analysis, because of the formation of a very stable sulfur-containing compound with Ce^{3+} ions tentatively ascribed[5] to oxysulfides (i.e., Ce_2O_2S) or sulfides (i.e., Ce_2S_3), considering literature data.[16,17] These compounds suggest that $Ce_2(SO_4)_3$ decomposes by another route in the presence of soot. Moreover, MS.s indicate that the amount of Ce^{4+} ions does not change during the He-TPE,[5] showing that the CeO_2 particles of the as-prepared soot are not affected significantly during the TPD. Whatever the route, the $Ce_2(SO_4)_3$ decomposition provides a large amount of oxygen species: 630, 1266, and 2532 μmol of O/g of soot, assuming the formation of Ce_2O_3, Ce_2O_2S, or Ce_2S_3, respectively. These oxygen species may react with the SOCs, leading to the CO_2 production in Figure 1, assuming a reaction such as

$$CO_{ads}\ (\text{SOC species}) + O\ (\text{linked to } Ce_xO_yS_z) \rightarrow CO_2 \qquad (7)$$

This is one of the expected impacts of the cerium additive: to favor the selectivity of the soot combustion into CO_2 (in agreement with the CO_2/CO ratio being ~3 during light-off tests[5]).

The aforementioned discussion leads to the view that the main difference in the He-TPE spectra of the as-

(27) Figueiredo, J. L.; Pereira, M. F. R.; Freitas, M. M. A.; Orfao, J. J. M. *Carbon* **1999**, *37*, 1379−1389.

prepared Cec-DS soot and those of nc-DS and Printex U is not linked to the nature of the SOCs. It comes from the oxidation of the stable SOCs, which are present whatever the soot, by the oxygen species provided by $Ce_xO_yS_z$.

4.2. O_2 Adsorption on the Three Soots at Several Temperatures. The O_2 chemisorption on carbon materials without additive to form SOCs is well-documented (ref 28 and references therein). There is a uniform adsorption activation energy (denoted by E_a) distribution: E_a linearly increases as the coverage increases[28] (i.e., from 4 kJ/mol to 120 kJ/mol).[28] This explains why the $Q_{O_2,ir}$ values of carbon materials increase (i) with the duration t_a of the adsorption at a constant T_a value and (ii) with the increase in T_a for a constant t_a value.[29] This is the situation on nc-DS and Printex U: E_a does not allow the adsorption of O_2 at T_a = 300 K (contrary to Cec-DS) and higher T_a values must be used. The adsorption of O_2 at 300 K on Cec-DS desorbed at 1100 K is mainly due to the $Ce^{3+} \rightarrow Ce^{4+}$ transformation.[5] This process is observed even at T_a = 173 K and P_{O_2} = 1 kPa, confirming the high reactivity of the reduced form of $Ce_xO_yS_z$ with O_2. For comparison, the partial reoxidation of Ce_2O_3 to CeO_2 at 300 K is only observed on highly dispersed particles,[30] whereas a temperature of 400 K is needed for the total oxidation of larger CeO_2 particles.[31] In parallel to the $Ce^{3+} \rightarrow Ce^{4+}$ transformation on Cec-DS for T_a = 300 K, there is a small production of SOCs: Q_{SOC} = 94 μmol/g, as compared to that of the as-prepared Cec-DS, suggesting that the SOCs are formed at the proximity of the $Ce_xO_yS_z$ particles. Moreover, Q_{SOC} for Cec-DS increases as T_a increases, as observed on conventional carbon materials, indicating that the O_2 chemisorption remains an activated process in the presence of $Ce_xO_yS_z$. The comparison of Q_{SOC} formed at 573 K (for nonsustained soot oxidation) on Cec-DS and nc-DS—568 (2.38 μmol/m^2) and 260 μmol/g (1.45 μmol/m^2), respectively—shows that the increase by a factor of ~2 on Cec-DS is not "spectacular". The O_2 adsorption at T_a = 660 K on Cec-DS leads to a Q_{SOC} value that is much smaller than that of the as-prepared soot. This suggests that either the interaction of $Ce_xO_yS_z$ with the soot is modified significantly by the He-TPE at 1100 K (i.e., sintering) or/and the Q_{SOC} value of the as-prepared Cec-DS is linked to the specific experimental conditions of the soot formation in the engine/exhaust line system (partial pressure of O_2 and temperature). However, the key result of the O_2 chemisorption on Cec-DS is that the profiles of the He-TPE spectra (see Figure 4) are identical to that of the "as-prepared" soot (see Figure 1), supporting the view that the same SOCs are formed (only their amounts are different). The He-TPD after O_2 adsorption at 660 K reveals a SO_2 production similar to that on the fresh Cec-DS, indicating that the stable $Ce_xO_yS_z$ compound is modified to a $Ce_2(SO_4)_3$-like compound.

A last comment on the O_2 adsorption/He-TPE cycle experiments concerns the SOCs formed at low adsorption temperatures. These very reactive SOCs that are formed on specific CC_f sites produce CO_2 during the He-TPE at T < ~700 K. However, these SOCs are irreversibly removed from the surface during oxidation (they are involved in the CO_2 production with the decreasing exponential profile in Figure 3). The initial CC_f sites are not regenerated by reaction 4, which may produce CC_f sites, forming more-stable SOCs. In the view of the microkinetic approach of the soot oxidation, this leads to the conclusion that only stable SOCs desorbing at T > ~700 K are involved in the sustained soot oxidation. This explains that the kinetic modeling of the He-TPE observations developed in the present study concerns the CO, CO_2, and SO_2 peaks desorbing at T > 700 K.

4.3. Kinetic Equations for the Modeling of the He-TPE Spectra on Cec-DS. Considering the aforementioned discussion, the kinetic modeling of the He-TPE of the as-prepared Cec-DS is based on the following views of the surface processes: (i) the stable SOCs on the as-prepared Cec-DS are similar to those on nc-DS and Printex U; (ii) $Ce_xO_yS_z$ particles are a reservoir of oxygen species that is available at the temperature of desorption/decomposition of these particles (detection of the SO_2 peak in Figure 1) to form very stable cerium oxysulfides/sulfides; and (iii) these oxygen species diffuse on the soot surface and oxidize the SOCs forming the characteristic CO_2 peak at T_m = 905 K (see Figure 1). This qualitative description of the surface processes is consistent with the "spill over" mechanism for the calcium-catalyzed gasification of carbon material,[32] and a comparison with this model is presented in a following section. Note that He-TPEs, after the adsorption of O_2 at T_a < 583 K (see Figure 4), show that the CO_2 peak is detected without any SO_2 production, indicating that several $Ce_xO_yS_z$ compounds may provide oxygen species. This is in agreement with the well-known oxygen storage capacity of CeO_2 that is used in three-way catalysis.[33] The characteristic CO_2 peak at T_M = 905 K is associated with a broad shoulder at T_M = 985 K (total amount of CO_2 is 2174 μmol/g). On nc-DS and Printex U,[5] there are similar broad CO_2 peaks, at ~950−1000 K, that are probably linked to the desorption of lactone or/and anhydride.[27] We may assume that these specific SOCs are also present on Ce-DS and desorb, in parallel with the CO_2 production that is due to the oxidation process, leading to the shoulder at 985 K in Figure 1. The exact profile of the two CO_2 peaks are not known and an approximate deconvolution gives ~574 μmol of CO_2/g for the desorption of SOCs and ~1600 μmol of CO_2/g for the oxidation process. According to these views, the following surface elementary steps are considered:

Step Sa: The cerium-containing particles provide oxygen species to the soot surface, according to

$$Ce_xO_yS_z \rightarrow O_s + Ce_xO_{y-1}S_z \quad \text{(with rate constant } k_{d,a} \text{ and activation energy } E_{d,a}) \tag{8}$$

This reaction can be summarized as $O_a \rightarrow O_s$, with O_a

(28) Perrichon, V.; Laachir, A.; Bergeret, G.; Fréty, R.; Tournayan L.; Touret, O. *J. Chem. Soc., Faraday Trans.* **1994**, *90*, 773−781.
(29) Feng, B.; Bhatia, S. K. *Chem. Eng Sci.* **2000**, *55*, 6187−6196.
(30) Isamil, I. M. K.; Walker, P. L., Jr. *Carbon* **1989**, *27*, 549−559.
(31) Putna, E. S.; Vohs, J. M.; Gorte, R. J. *Catal. Lett.* **1997**, *45*, 143−147.
(32) Tomita, A. *Catal. Surveys Jpn.* **2001**, *5*, 17−24.
(33) Duprez, D.; Descorme, C. Oxygen Storage/Redox Capacity and Related Phenomena on Ceria-Based Catalysts. In *Catalysis by Ceria and Related Materials*; Trovarelli, A., Ed.; Imperial College Press: London, 2002; p 243.

being the oxygen species at the surface of the $Ce_xO_yS_z$ particles. According to the view of the "spill over" mechanism,[32] the O_s species diffuse on the soot surface at some distance of $Ce_xO_yS_z$.

Step Sb: The O_s species react with the stable SOCs that are present on the as-prepared Cec-DS to form CO_2:

$$C_nCC_fO + O_s \rightarrow CO_2 + C_{n-1}CC_f$$

(with rate constant k_O and activation energy E_O) (9)

Step Sc: Similar to conventional carbon materials,[18−27] the stable SOCs species involved in step Sb desorb as CO (and/or CO_2):

$$C_nCC_fO \rightarrow CO + C_{n-1}CC_f \quad (10a)$$

or

$$C_nC(O)C_f(O) \rightarrow C_{n-1}CC_f + CO_2 \quad (10b)$$

where the rates constant $k_{d,SOC}$ and the activation energy $E_{d,SOC}$ of reactions 10a and 10b differ for each SOC present on the soot surface. Literature data indicate that TPD of SOCs on carbon materials frequently leads to the observation of broad peaks on a large range of temperature, because of strongly overlapped CO and CO_2 peaks.[18−27] These broad peaks that cannot be deconvoluted to evaluate the $E_{d,SOC}$ values of reaction 10a or 10b for each individual SOC. However, an average of the activation energies of desorption of the SOCs can be obtained from those broad peaks, assuming an increase in $E_{d,SOC}$ with the decrease in the coverage θ_{SOC} of the SOCs. This means that, to simulate the desorption of several SOCs from a soot surface, one has the choice of considering either several steps (reactions 10a and/or 10b) with an activation energy of desorption that is independent of θ_{SOC} or a limited number of those steps with averaged activation energies of desorption, depending on θ_{SOC} (i.e., for simplicity, a linear variation of $E_{d,SOC}$ with θ_{SOC}). To facilitate the presentation, a single step (reaction 10a) with an activation energy of desorption that increases as θ_{SOC} decreases is involved in the first stage of the kinetic modeling, then in a second stage, several steps (reactions 10a and 10b) are considered.

We use $[O_a]$, $[O_s]$, and $[C_fO]$ to represent the surface concentrations (in units of molecules/cm^2) of the O_a, O_s, and SOCs of the as-prepared Cec-DS soot. Steps Sa−Sc lead to the following set of equations:

$$-\frac{d[O_a]}{dt} = k_{d,a}[O_a] \quad (11)$$

$$\frac{d[O_s]}{dt} = k_{d,a}[O_a] - k_O[O_s][C_fO] \quad (12)$$

$$\frac{d[C_fO]}{dt} = k_{d,SOC}[C_fO] + k_O[O_s][C_fO] \quad (13)$$

In expressions 11−13, the units of the rate constants are s^{-1} for $k_{d,a}$ and $k_{d,SOC}$ and (cm^2 molecule^{-1} s^{-1}) for k_O. The total amounts of CO_2 and CO formed during the He-TPE (4608 μmol/g) and the BET surface area give an evaluation of the highest surface concentration of the SOC species on the soot: $[C_fO]_M \approx 19.3$ μmol/m^2 $\approx 10^{15}$ molecules/cm^2. The ratio $[C_fO]/[C_fO]_M$ corresponds to the coverage of the SOCs at time t, denoted as θ_{SOC} (at time 0: $\theta_{SOC}(0) = 1$). Dividing expressions 11−13 by $[C_fO]_M$ leads us to define $[O_s]/[C_fO]_M$ and $[O_a]/[C_fO]_M$ as the apparent coverages (relative of the SOC content of the soot), denoted as θ_{a,O_s} and θ_{a,O_a}, respectively. This leads to

$$-\frac{d\theta_{a,O_a}}{dt} = k_{d,a}\theta_{a,O_a} \quad (14)$$

$$\frac{d\theta_{a,O_s}}{dt} = k_{d,a}\theta_{a,O_a} - k_O[O_s]\theta_{SOC} \quad (15)$$

$$\frac{d\theta_{SOC}}{dt} = k_{d,SOC}\theta_{SOC} + k_O[O_s]\theta_{SOC} \quad (16)$$

Considering the contribution of the SOC oxidation (reaction 9) to the CO_2 production at $T_M = 905$ K in Figure 1 (1600 μmol/g), it is determined that $\theta_{a,O_a}(0) \approx 0.35$ at time $t = 0$. The pre-exponential factors of $k_{d,a}$ and $k_{d,SOC}$ are considered equal to the theoretical value for either a desorption or a decomposition of the first kinetic order: $\sim 10^{13}$ s^{-1}. Considering the literature data, Du et al.[19] have discussed the values of this parameter for SOCs and they recommend using a value of 10^{13} s^{-1} if no better values are available. Moreover, Haydar et al.[24] have determined (using ITPD) that the pre-exponential factors for the desorption rate constants of several SOCs species are in the range of $10^{11}-10^{14}$ s^{-1} (the highest value of this parameter[19] is considered to be equal to the vibration frequency of diamond: 2.5×10^{14} s^{-1}). Similarly, k_O corresponds to the rate constant of a Langmuir−Hinshelwood (L−H) elementary step with a theoretical pre-exponential factor of $\sim 10^{-2}$ cm^2 molecule^{-1} s^{-1}.[34,35] Considering that $[C_fO]_M \approx 10^{15}$ molecules/cm^2, then one obtains $k_O[O_s] = k_O[C_fO]_M\theta_{a,O_s} = k_{a,O}\theta_{a,O_s}$, with a pre-exponential factor of $k_{a,O} \approx 10^{13}$ s^{-1}, as used in gas/solid heterogeneous catalysis for a L−H step.[36−38] The final expressions for the kinetic modeling of the He-TPE experiments are as follows:

$$-\frac{d\theta_{a,O_a}}{dt} = k_{d,a}\theta_{a,O_a} \quad (17)$$

$$\frac{d\theta_{a,O_s}}{dt} = k_{d,a}\theta_{a,O_a} - k_{a,O}\theta_{a,O_s}\theta_{SOC} \quad (18)$$

$$\frac{d\theta_{SOC}}{dt} = k_{d,SOC}\theta_{SOC} + k_{a,O}\theta_{a,O_s}\theta_{SOC} \quad (19)$$

The set of equations (eqs 17−19) allows one to simulate the evolutions of the coverages of the different species in the course of the He-TPE ($dT/dt = \beta$). These curves provide the evolutions of the rates of the CO_2 and CO

(34) Rinnemo, M.; Kulginov, D.; Johansson, S.; Wong, K. L.; Zhadanov, V. P.; Kasemo, B. *Surf. Sci.* **1997**, *376*, 297.
(35) Campbell, C. T.; Ertl, G.; Kuipers, H.; Segner, J. *J. Chem. Phys.* **1980**, *73*, 5862−5873.
(36) Glasstone, S.; Laidler, K. J.; Eyring, H. *The Theory of Rate Processes*; McGraw-Hill: NewYork, 1941.
(37) Herz, R. H.; Marin, S. P. *J. Catal.* **1980**, *65*, 281−296.
(38) Oh, S. H.; Fisher, G. B.; Carpenter, J. E.; Goodmann, D. W. *J. Catal.* **1986**, *100*, 360−376.

Table 2. Experimental Parameters for He-TPE

parameter	value
radius of the reactor, R_r (cm)	0.72
volume of the reactor, V_r (cm^3)	1.1
weight of catalyst, W_c (g)	~0.2
particle size, R_p (cm)	0.02
particle density, ρ (g/cm^3)	
slightly compressed	0.46
before compression	0.14
particle porosity (slightly compressed), ϵ_p	0.7
gas flow rate, f (cm^3/min)	100
heating rate, β (K/min)	50

productions R_{CO_2} and R_{CO}, respectively, relative to the desorption temperature, according to reactions 9 and 10:

$$R_{CO_2} = k_{a,O}\theta_{a,O_s}\theta_{SOC} \quad (20)$$

$$R_{CO} = k_{d,SOC}\,\theta_{SOC} \quad (21)$$

4.4. Kinetic Modeling of the He-TPE Spectrum of the As-Prepared Cec-DS. The intent of the modeling is to simulate, using eqs 17−21, the He-TPE spectra of the as-prepared Cec-DS soot (Figure 1) in particular, regarding the temperatures at the maximum of the CO, CO_2, and SO_2 peaks.

4.4.1. On the Validity of the Kinetic Modeling of the He-TPE Observations. The exploitation of He-TPE data for the determination of the kinetic parameters of surface elementary steps forces us to assert that the experimental conditions prevent the impact of different processes such as lags, diffusion, and readsorption. For a TPD procedure using a carrier gas flow passing through a bed of catalyst particles, Demmin and Gorte[39] have defined six dimensionless criteria Cr_i, which allows one to evaluate the impacts of convective (Cr_1) and diffusive (Cr_2) lags, particles (Cr_3) and bed (Cr_4) concentration gradients, and readsorption at high (Cr_5) and low (Cr_6) flow rates. The practice of those criteria[40,41] (they must be less than ~0.01−1) reveals that it is easy to design experimental conditions that prevent the lags, whereas gradient concentrations in the particles and in the bed are more stringent to be respected, imposing a careful design of the experiment. Table 2 gives the parameters of interest to evaluate the Cr_1−Cr_4 Demmin and Gorte criteria for the present experimental conditions with bed and particle diffusion coefficients of 1 and 0.01 cm^2/s, respectively, as used by other authors[40,41] for similar experimental conditions (see refs 39−41 for more details on the calculation of Cr_i and the discussion of their values). The Cr_6 and Cr_5 values are dominated by two factors:[39] (a) $F = [RT/(2\pi M)]^{1/2} > \sim 100$ m/s, which comes from the adsorption rate constant, and (b) the surface area per unit volume. For nonactivated chemisorption such as CO and H_2 on metal-supported catalysts, the Cr_5 and Cr_6 values are $\sim 10^5 \gg 1$, indicating that classical TPD experiments are performed under quasi-equilibrium conditions,[39−41] allowing the experimental data to be treated by particular mathematical formalisms.[40,41] The TPD and He-TPE of SOCs adsorbed on carbon material is a particular situation for readsorption, because of the fact that O_2, CO, and CO_2 chemisorptions are strongly activated processes at high θ_{SOC} values. Several studies have shown that the values of the activation energy of oxygen adsorption increase with the SOCs coverage in a very large range of 4−150 kJ/mol.[28,42,43] On Cec-DS, the results in Figures 3−5 clearly show that the O_2, CO, and CO_2 chemisorptions are activated processes. Moreover, in Figure 1, CO and CO_2 peaks formed during the He-TPE for $T > 650$ K come from a surface widely covered by SOCs associated with high E_a values, which, in turn, strongly decreases the rate of adsorption. For an activated chemisorption, the factor F must be multiplied by $\exp[-E_a/(RT)]$, which strongly decreases the Cr_5 and Cr_6 values. The activation energies of adsorption of CO and CO_2 on the present Cec-DS are not known. However, it is easy to determine the values of E_a that lead to Cr_5 and Cr_6 values of <1 (an absence of readsorption) at 900 K (the temperature of the main CO_2 peak in Figure 1): $E_a \geq 140$ kJ/mol. This value is reasonable for a high coverage of the surface.[28,42,43] Moreover, Demmin and Gorte[39] have used the mathematical formalism of the kinetic theory of gases to express the rate of adsorption. The mathematical formalism of the activated complex theory (ACT) leads to a different expression for the rate of adsorption, and simple calculations show that the kinetic theory of gases leads to a pre-exponential factor of the rate constant of adsorption that is higher by a factor of ~2000 at 900 K, as compared to ACT. This means that, using the ACT approach, Cr_5 and Cr_6 can be <1 for activation energies of adsorption of $E_a \geq 80$ kJ/mol, which (i) increases the validity of the criteria on a larger coverage range of SOCs and (ii) significantly reinforces the view that readsorption of CO and CO_2 at high coverages of the soot are negligible at $T \approx 900$ K, as considered in the present study.

4.4.2. Simulation of the He-TPE Spectrum on Cec-DS. To obtain a theoretical He-TPE profile in agreement with the experimental data (Figure 1), the procedure consists of determining the best set of activation energies for the three elementary steps (Sa−Sc). Literature data on the TPD of SOCs on various carbon materials show that, at $T_d > 600$ K, there is a broad CO peak with more-or-less discernible shoulders.[18−27] These profiles are used to determine $E_{d,SOC}$ (step Sc), according to two options: either a distribution function for $E_{d,SOC}$ with the coverage of the soot surface[19] or a deconvolution in several individual peaks is performed, leading to a set of increasing $E_{d,SOC}$ values.[24] However, the authors[24] note that the theoretical TPD profile obtained using the experimental $E_{d,SOC}$ and pre-exponential values is more resolved than the experimental profile (the $E_{d,SOC}$ value for a particular SOC is rarely independent of the coverage). In the first stage of the present modeling, we consider that $E_{d,SOC}$ increases linearly as the coverage decreases, according to

$$E_d(\theta_{SOC}) = E_d(1) + \alpha(1 - \theta_{SOC})$$

where $E_d(1)$ is the activation energy at full coverage ($E_d(1) = 260$ kJ/mol) and $\alpha = 70$ kJ/mol (these values are consistent with the literature data[24]). As mentioned

(39) Demmin, R. A.; Gorte, R. J. *J. Catal.* **1984**, *90*, 32−39.
(40) Efsthathiou, A. I.; Bennett, C. O. *J. Catal.* **1990**, *124*, 116−126.
(41) Derrouiche, S.; Bianchi, D. *Langmuir* **2004**, *20*, 4489−4497.
(42) Floess, J. K.; Lee, K. L.; Oleksy, S. A. *Energy Fuels* **1991**, *5*, 133−138.
(43) Teng, H.; Hsieh, C. T. *Ind. Eng. Chem. Res.* **1999**, *38*, 292−297.

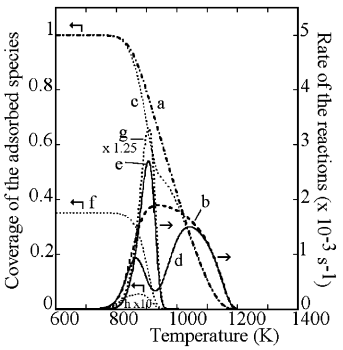

Figure 7. Theoretical He-TPE spectra of the as-prepared Cec-DS soot, according to the kinetic modeling (see text for more details): (a) coverage of the SOC in the absence of additive; (b) CO production in the absence of additive; (c) coverage of the SOC in the presence of the $Ce_xO_yS_z$; (d) CO production in the presence of the $Ce_xO_yS_z$; (e) CO_2 production in the presence of the $Ce_xO_yS_z$; (f) coverage of the O_a species in the presence of additive; (g) the rate of decomposition of the $Ce_xO_yS_z$ particles; and (h) coverage of the soot by oxygen species, considering an activation energy for the SOC oxidation of 230 kJ/mol.

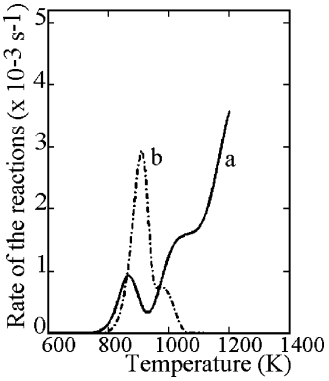

Figure 8. Theoretical He-TPE spectra, considering that the CO and CO_2 peaks are due to the oxidation and desorption of different SOC species: (a) CO and (b) CO_2.

in the previous section, this represents an average of the activation energy of desorption of several SOCs species, providing a broad CO peak during TPD. For instance, curves a and b in Figure 7 show the evolutions of θ_{SOC} and the rate of CO production, respectively, during the desorption of SOC in the absence of the cerium additive (only step Sc is considered); curve b mimics a strong overlap of several CO peaks. Curves c, d, and e in Figure 7 shows the evolutions of θ_{SOC} and the rate of CO and CO_2 productions, respectively, during the He-TPE of the SOCs in the presence of $Ce_xO_yS_z$, considering that E_O = 230 kJ/mol and $E_{d,a}$ = 260 kJ/mol in eqs 17−21. Curves f and g in Figure 7 give the evolutions of θ_{a,O_a} and the rate of the O_s production (corresponding to the rate of the $Ce_xO_yS_z$ decomposition), whereas curve h gives the evolution of θ_{a,O_s} (the coverage of the soot by oxygen species). The temperatures at the maximum of the theoretical peaks in Figure 7 are consistent with the experimental observations in Figure 1: T_M = 907 K for CO_2 and T_M = 865 K and T_M = 1050 K for the two CO peaks (the experimental values in Figure 1 are 905, 864, and 1100 K, respectively). This shows that the CO and CO_2 peaks in Figure 1 do not indicate the presence of different SOCs. They are due to the fact that the rate of oxidation of the SOCs is higher than their rate of desorption (characterized by $E_d(\theta_{SOC}) = f(\theta_{SOC})$) as soon as some O_s species are available, because of the desorption/decompositon of $Ce_xO_yS_z$. To respect the experimental observations (T_M values), the rate of the desorption at low temperatures must be similar to the rate of the desorption/decomposition of $Ce_xO_yS_z$. Considering that, at the beginning of the SOCs desorption, the cerium is present as $Ce_2(SO_4)_3$, curve g in Figure 7 must correspond to the rate of the SO_2 production, considering reaction 6. In Figure 7, curve g is overlapped with the CO_2 production (curve e) and the T_M value does not correspond to that in Figure 1. This is probably linked to the complexity of the evolution of the $Ce_xO_yS_z$ composition during the He-TPE in the presence of soot. At low temperatures, the decomposition of $Ce_2(SO_4)_3$ must be considered with the formation of SO_2 (as in the absence of soot[5]) with a production of CeO_2 (or its reduced form, Ce_2O_3). The route of the decomposition then changes with the increase in temperature, forming the very stable Ce_2O_2S-like compound[5] without SO_2 production. This explains that the SO_2 production ceases in Figure 1 for $T > \sim 770$ K, whereas the O_s production continues for the SOC oxidation (oxygen species are available without any SO_2 production). The E_O value of 230 kJ/mol in Figure 7 has been selected because it leads to small θ_{a,O_s} values (see curve h in Figure 7). However, E_O values of <230 kJ/mol do not modify the CO_2 and CO peaks in Figure 7: only θ_{a,O_s} decreases (results not shown). This shows that it is not step Sb that controls the CO_2 production in Figure 1.

The simulation in Figure 7 does not exactly correspond to the observation in Figure 1, because of the absence of the CO and CO_2 shoulders at 1100 and 985 K, respectively. To mimic those shoulders, we assume in a second stage of the kinetic modeling that there are, in addition to the oxidation of the SOCs (denoted $SOCs_0$, characterized by $E_d(\theta_{SOC}) = 260 + 70(1 - \theta_{SOC})$), (i) SOCs (denoted $SOCs_1$) desorbing as CO with an activation energy higher than that of $SOCs_0$ and (ii) SOCs (denoted $SOCs_2$) desorbing as CO_2 in parallel with the oxidation (new steps (reactions 10a and 10b) are introduced in the kinetic model). Figure 8 gives the new profile, considering (i) for SOC_1, $E_d(1)$ = 350 and α = 20 kJ/mol; (ii) for SOC_2, $E_d(1)$ = 210 kJ/mol and α = 80 kJ/mol; and (iii) the ratio between the amount of the three SOCs is $SOC_0/SOC_1/SOC_2$ = 1/1/0.15.

4.5. Comparison of the Kinetic Parameters Used in the Kinetic Modeling to Literature Data. The theoretical curves in Figures 7 and 8 give a reasonable interpretation of the characteristic features in Figure 1 for a specific set of activation energies: namely, for SOC_0, $E_{d,SOC} = 230 + 70(1 - \theta_{SOC})$ kJ/mol and $E_O <$ 230 kJ/mol; and for the decomposition of $C_xO_yS_z$, $E_{d,a}$ = 260 kJ/mol. Moreover, the kinetic modeling does not consider that the surface diffusion of O_s species contribute to the He-TPE spectra. These conclusions are compared to the literature data.

4.5.1. Desorption of the SOCs. The $E_{d,SOC}$ values are consistent with those determined by several authors, using a pre-exponential factor of 10^{13} s^{-1} (see ref 24 and references therein) for the desorption of SOCs as CO at $T > 600$ K. A lower pre- exponential, such as 10^{11} s^{-1}, leads to $E_{d,SOC}$ values that are smaller, by ~40 kJ/mol, as compared to that obtained using 10^{13} s^{-1}.[24] The point of interest is that the use of an $E_d(1)$ value of >260 kJ/

mol in the kinetic modeling leads to suppression of the first CO peak (a larger fraction of SOCs is oxidized), whereas using $E_d(1)$ values of <260 kJ/mol reinforces and shifts the first CO peak to lower temperatures (a larger fraction of SOCs desorbs before the oxygen is available). These two situations do not correspond to the experimental observations, showing that the $E_{d,SOC}$ values for the SOCs oxidized by the oxygen species coming from the additive must be selected in a very short range of values.

4.5.2. Oxidation of the SOCs. For E_O, the simulation only provides an upper limit: 230 kJ/mol (lower values have no impact on the CO and CO_2 peaks in Figure 7). These values can be only compared to the apparent activation energy $E_{a,O}$ for the oxidation of soots. In a review article, Stanmore et al.[1] noted that the literature data on $E_{a,O}$ cover a range of 102−210 kJ/mol, with a large number of studies providing values in the range of 140−170 kJ/mol. The authors[1] suggested that the low values could be related to specific experimental conditions. Du et al.[44] determined that the $E_{a,O}$ values of noncatalyzed and calcium-catalyzed soot are 142 and 121 kJ/mol, which are consistent with the view that the catalyst does not change the kinetic mechanism profoundly.[2] Recent literature data confirm that the $E_{a,O}$ values are in the range of 140−170 kJ/mol, such as 157−164 kJ/mol (from the work of Dernaika and Uner[45]) and 164 kJ/mol (from the work of Higgins et al.[46]), which are consistent with the value observed for the oxidation of Printex U (170 kJ/mol).[3] Higgins et al.[46] have shown that the activation energy is not modified by the size of the soot particles, whereas the pre-exponential factor is slightly affected (by a factor of ~1.7).[46]

4.5.3. Desorption/Decomposition of the $Ce_xO_yS_z$ Particles. The kinetic order and the activation energy of decomposition (260 kJ/mol) used for the production of O_s (from the decomposition of $Ce_xO_yS_z$) are compared to data from the study of Ying and Rudong[47] on the decompositon of pure cerium sulfate. Using the method developed by Freeman and Caroll,[48] the authors have estimated an activation energy of 298.4 kJ/mol and an kinetic order of 0.383 for the decomposition of $Ce_2(SO_4)_3$, according to[47]

$$Ce_2(SO_4)_3 \rightarrow 2CeO_2 + 2SO_3 + SO_2 \qquad (22)$$

However, in Part I,[5] the decomposition of pure $Ce_2(SO_4)_3$, according to a procedure similar to the present He-TPE conditions, has led to the observation of two simultaneous SO_2 and O_2 peaks with a ratio that is in agreement with reaction 6.[49,50] A kinetic modeling of this production during the decomposition of pure sulfate has been performed considering first-order kinetics with a pre-exponential factor of 10^{13} s^{-1}. Figure 9 shows that very good agreement exists between the kinetic modeling and the experimental data, considering an activation energy of desorption of 330 kJ/mol, which is consistent with the value of Ying and Rudong.[47] However, this value is significantly higher than that used in the kinetic modeling of the He-TPE (260 kJ/mol). One must consider that either the $Ce_xO_yS_z$ particle size or/and the interactions between the $Ce_2(SO_4)_3$ and the soot significantly decrease the activation energy of decomposition of the well-dispersed $Ce_xO_yS_z$ particles. Moreover, it must be considered that this decomposition only follows reaction 6 at the beginning of the process, because of the final formation of the very stable cerium oxysulfides and sulfides.

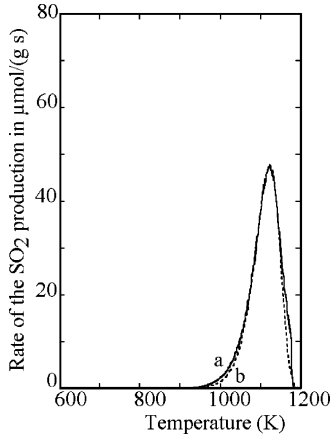

Figure 9. Experimental and theoretical rates of decomposition of pure $Ce_2(SO_4)_3$ during TPD (see text for more details); experimental data is represented by the continuous line (curve a), and the theoretical profile is represented by the dotted line (curve b).

4.5.4. Surface Diffusion of the O_s Species. The present kinetic modeling of the He-TPE of Cec-DS is consistent with the "spill-over model" of the soot oxidation.[32] It is of interest to (i) evaluate how far the O_s species must diffuse from the $Ce_xO_yS_z$ particles to oxidize the 1600 μmol/g of SOCs and (ii) compare the rate of the O_s diffusion on the soot surface to the rate of oxidation of the SOCs. MS.s have indicated that 49% of the cerium content of Cec-DS is present as Ce^{3+} of the cerium sulfate, corresponding to 212 μmol of $Ce_2(SO_4)_3$/g of soot. XRD analysis has only revealed the presence of CeO_2 particles (average diameter of 23 nm),[5] indicating that the $Ce_2(SO_4)_3$ is present as well-dispersed particles (i.e., particle sizes of less than ~3 nm). Assuming hemispherical particles with a diameter of 2 nm and considering that the density of the $Ce_xO_yS_z$ particles is equal to that of ceria (CeO_2)—7.132×10^3 kg/m^3—then simple calculations allow one to determine (i) the number of $Ce_2(SO_4)_3$ particles on the soot (3.4×10^{16} particles/m^2 of soot), (ii) the surface area of the soot covered by these particles (25.2 m^2/ g of soot, as compared to the BET area of the soot (239 m^2/g)), and (iii) the surface of the soot around the $Ce_xO_yS_z$ particles that contain the SOCs that have been oxidized during the He-TPE (1600 μmol/g). The calculations indicate that the SOCs are contained on a surface at a distance of ~3 nm from the cerium-containing particles: this value represents the highest diffusion distance for the O_s species (larger $Ce_xO_yS_z$ particles increase this distance). Surface diffusion of the O_s species can be estimated from the model that was developed by Kramer and Andre[51] for the hydrogen spillover from platinum particles that were

(44) Du, Z.; Sarafin, A. F; Longwell, J. P. *Energy Fuels* **1991**, *5*, 214−221.
(45) Dernaika, B.; Uner, D. *Appl. Catal., B* **2003**, *40*, 219−229.
(46) Higgins, K. J.; Jung, H.; Kittelson, D. B.; Roberts, J. T.; Zachariah, M. R. *J. Phys. Chem. A* **2002**, *106*, 96−103.
(47) Ying, Y.; Rudong, Y. *Thermochim. Acta* **1992**, *202*, 301−306.
(48) Freeman, E. S.; Carroll, B. *J. Phys. Chem.* **1958**, *62*, 394−397.
(49) Poston, J. A., Jr.; Siriwardane, R. V.; Fisher, E. P.; Miltz, A. L. *Appl. Surf. Sci.* **2003**, *214*, 83−102.
(50) Flouty, R.; Adi-Aad, E.; Siffert, S.; Aboukaïs, A. *J. Therm. Anal. Calorim.* **2003**, *73*, 727−734.

randomly distributed on an alumina support. Considering reasonable simplifications, the amount of species diffused from a circular source (of radius a) to 1 cm^2 of support is given by[51]

$$c = \frac{4NaC_e}{\sqrt{\pi}}\sqrt{Dt} \qquad (23)$$

where N is the number of metal particles per square centimeter of support, C_e the surface concentration in the source (given in units of atoms/cm^2), and D the coefficient of surface diffusion of the hydrogen species on the support. This model can be applied to different situations such as for the diffusion of oxygen species from the metal particles to the support.[52] To support the present kinetic modeling that does not consider the rate of diffusion of O_s, the amount of O_s diffused on the soot for a given time of reaction must be significantly higher than that need to oxidize the soot: 1600 μmol/g of soot or 6.8×10^{-4} μmol/cm^2 of soot. The diffusion coefficient D of the O_s species on the soot surface is not known. However, considering a large review of literature data, Seebauer and Allen[53] have shown that the values of $D = D_0 \exp[-E_{diff}/(RT)]$ are not very different on various surface materials, and in the temperature range of the present experiments, a value of $D = 5 \times 10^{-13}$ cm^2/s seems reasonable.[53] Assuming a surface concentration of O_a species on the $Ce_xO_yS_z$ particles of 10^{14} atoms/cm^2, expression 23 indicates that the amount of O_s needed for the SOC oxidation are available after $t < 10$ s; this value is significantly lower than that corresponding to the SOC oxidation. These calculations support the view that the diffusion of O_s on the soot has no significant impact on the He-TPE observations.

4.6. The Contribution of the He-TPE Modeling to the Study of the Oxidation of Diesel Soots. The kinetic modeling of the He-TPE observations is an element of the microkinetic approach of the Cec-DS oxidation, because the elementary steps Sa−Sc must be operative during the sustained soot oxidation. The simulations in Figures 7 and 8 clearly show that stable SOCs species (similar to noncatalyzed soot) formed by adsorption of O_2 on the soot in the engine/exhaust line system are preferentially oxidized at $T > 700$ K by the oxygen species coming from the desorption/ decomposition of the cerium-containing particles. The kinetic modeling shows that, during the He-TPE, it is the activation energy of this decomposition and not that of oxidation of the SOCs that controls the CO_2 production. These elements of the microkinetic approach of the soot oxidation can be compared to the literature data on the elementary steps considered for the catalytic oxidation of carbon materials.

4.6.1. Comparison of the Present Kinetic Modeling to Calcium-Catalyzed Gasification of Carbon. Tomita[32] recently summarized the views of the surface processes for the calcium-catalyzed gasification of carbon materials, considering, in particular, experiments that were performed with $^{18}O_2$ and $^{16}O_2$ on nondoped and calcium-doped graphite surfaces (denoted G and Ca-G, respectively).[54] It is mainly considered[32,54] that the adsorption of O_2 on CaO particles forms adsorbed oxygen species (denoted CaO(O)) that supply oxygen to the carbon surface at a very fast rate (in agreement with the aforementioned calculations). On a soot surface that has been desorbed at 1300 K, these oxygen species (i) form SOCs with C_nCC_f sites (reaction 1) and (ii) oxidize the SOCs with the regeneration of a $C_{n-1}CC_f$ site (reactions 3 and 4). This explains why CaO favors the CO_2/CO ratio during oxidation, as compared to noncatalyzed carbon materials. The experiments with ^{18}O show that a large amount of $C_nCC_f(^{18}O)$ species remains on the soot surface after several minutes of gasification with $^{16}O_2$.[32,54] This indicates that carbon gasification occurs only in the vicinity of the CaO particles.[54] Thus, only a very small fraction of the SOCs participate to the CO_2 production, which is consistent with the highest diffusion distance of the O_s species (~3 nm). Finally, the kinetic modeling of the He-TPE experiments on Cec-DS, according to steps Sa−Sc, is consistent with the description of the gasification by O_2 of a calcium-catalyzed carbon surface:[32] the cerium-containing particles provide oxygen species (step Sa) to the soot surface that oxidize preadsorbed SOCs (step Sb) until the available oxygen species in $Ce_xO_yS_z$ are worked out. However, they are some differences in the two catalytic processes, as revealed by a comparison of the observations on Ca-G and Cec-DS during heating in an inert atmosphere. Kyotani et al.[49] compared the CO and CO_2 peaks after the gasification of Ca-G by O_2 at 900 K, followed by either a desorption at 900 K or a cooling stage in O_2 to 300 K (Figure 5 in ref 54). The point of interest is that cooling in O_2 mainly increases the amount of SOCs desorbing as CO, according to a peak at 980 K (small CO_2 peaks at $T_d < 900$ K are ascribed to the desorption of CO_2 from $CaCO_3$ formed by the adsorption of CO_2 on CaO during the cooling stage). This shows clearly that, in the absence of an oxygen partial pressure P_{O_2}, the CaO particles are not an oxygen reservoir to form CO_2 during the increase in temperature at the difference of the $Ce_xO_yS_z$ on Cec-DS. The main characteristic of the Cec-DS system, as compared to Ca-G, is that the oxygen species from the $Ce_xO_yS_z$ particles, oxide the SOCs in the absence of O_2. Note that He-TPEs on Cec-DS strongly support the idea that O_s species and not O_2 are involved in the oxidation process (step Sa). For instance, we may adopt the view that the decomposition of $Ce_2(SO_4)_3$ on the soot obeys reaction 6 and provides O_2 and not O_s. However, this situation does not allow us to establish a difference in the mechanism of the catalyzed and noncatalyzed soot at the opposite to the observations, in particular, on the CO_2/CO ratios during light-off test.[5]

4.6.2. Cerium-Catalyzed Soot Oxidation. The O_2 adsorption experiments on Cec-DS desorbed at $T > 1100$ K have revealed the high reactivity of the reduced form of $Ce_xO_yS_z$ (the reoxidation is observed at 173 K). This leads to the view that, during the oxidation of the soot in the presence of O_2, the $Ce_xO_yS_z$ particles constitute an infinite reservoir of O_s species (step Sa) as soon as the decomposition of the $Ce_2(SO_4)_3$ begins. It has been previously shown that the decomposition of $Ce_2(SO_4)_3$

(51) Kramer, R.; André, M. *J. Catal.* **1979**, *58*, 287−295.
(52) Descorme, C.; Duprez, D. *Appl. Catal., A* **2000**, *202*, 231−241.
(53) Seebauer, E. G.; Allen, C. E. *Prog. Surf. Sci.* **1995**, *49*, 265−330.
(54) Kyotani, T.; Hayashi, S.; Tomita, A. *Energy Fuels* **1991**, *5*, 683−688.

is not modified in the presence of O_2.[5] According to the kinetic modeling used in Figures 7 and 8, this means that the available O_a species (and, therefore, θ_{a,O_a}, increases in the presence of P_{O_2}. For instance, with the kinetic parameters used to obtain Figure 7, it is observed that the second CO peak is suppressed for $\theta_{a,O_a} = 1$: the SOCs are totally oxidized. This allows explanation of why the ratio CO_2/CO, during a light-off test with Cec-DS, is very high: ~3, compared to ~1 on nc-DS.[5] The P_{O_2} value favors the SOCs oxidation, because the $Ce_xO_yS_z$ particles become an infinite reservoir of O_s species and the CO production is limited to (i) the SOC desorption as CO before the decomposition of the sulfates (the first CO peak in Figure 7) and (ii) the desorption of the SOC as CO in parallel with their oxidation, which is due to the high and fast light-off exothermic processes ($\Delta T \approx 200$ K).[5] The present kinetic modeling fixes an upper limit for the activation energy of oxidation of the SOC: $E_O = 230$ kJ/mol (lower values have no impact on the CO and CO_2 peaks). This conclusion leads to the view that the ignition of a diesel soot can be decreased significantly if oxygen species are available at a lower temperature, using an additive that forms less-stable particles.

5. Conclusion

The intentions of the present study, in the view of a microkinetic approach of the oxidation of a cerium-catalyzed diesel soot formed in a engine/exhaust line, were (i) to study the reactivity of the surface-oxygenated complexes (SOCs) in the presence of $Ce_xO_yS_z$ particles using temperature-programmed experiments that applied a helium flow (He-TPE) and (ii) to provide a kinetic modeling of the observations.

As compared to noncatalyzed soot, the He-TPE profile of a Cec-DS is characterized by a CO_2 peak at $T_M = 905$ K between two CO peaks at $T_M = 864$ K and $T_M = 1100$ K. It has been shown, using O_2 chemisorption on the soot desorbed at 1100 K, that this He-TPE profile is not due to the desorption of specific SOCs formed during the formation of the soot. It is due to the oxidation of stable SOCs (also present on a noncatalyzed soot) by oxygen species provided by the decomposition of the $Ce_xO_yS_z$ particles. The kinetic modeling has shown that it is this decomposition that controls the CO_2 formation, rather than the oxidation of the SOCs. The comparison with literature data has shown that the kinetic modeling is consistent with the views of calcium-catalyzed carbon material. However, the particularity of Cec-DS is that the $Ce_xO_yS_z$ particles are an oxygen reservoir for the oxidation of SOCs, even in the absence of O_2, which explains the high CO_2/CO ratio that is observed during light-off tests.

EF049840F